Ab initio density functional theory study of strain effects on ferroelectricity at PbTiO3 surfaces

AUTHOR(S):

Umeno, Y; Shimada, T; Kitamura, T; Elsasser, C

PHYSICAL REVIEW B **74**, 174111 (2006)

Ab initio density functional theory study of strain effects on ferroelectricity at $PbTiO_3$ surfaces

Yoshitaka Umeno,[1,2] Takahiro Shimada,[2] Takayuki Kitamura,[2] and Christian Elsässer[1,3]
[1]*IZBS, University of Karlsruhe, Kaiserstrasse 12, 76131 Karlsruhe, Germany*
[2]*Graduate School of Engineering, Kyoto University, Sakyo-ku, Kyoto 606-8501, Japan*
[3]*Fraunhofer Institute for Mechanics of Materials IWM, Wöhlerstrasse 11, 79108 Freiburg, Germany*
(Received 13 August 2006; revised manuscript received 1 October 2006; published 15 November 2006)

The $PbTiO_3$ (001) surface structure with ferroelectric (FE) polarization parallel to the surface and its response to tangential strain have been studied using *ab initio* density functional theory calculations with the local density approximation. We find [110]-oriented ferroelectricity is more stable than [100]-oriented under zero and nonzero strain in both TiO_2 and PbO terminations. Tensile strain enhances the FE distortion and suppresses the antiferrodistortive rotation, while the opposite trend is found under compression. The FE polarization direction alters with respect to the variation of the uniaxial strain owing to the preference of the polarization along the longer axis of rectangular lattices. The sensitivity of the FE rotation significantly differs depending on the layer at PbO-terminated $c(2\times2)$ surface, leading to the variation of polarization directions among the layers under uniaxial strain.

DOI: 10.1103/PhysRevB.74.174111 PACS number(s): 77.55.+f, 77.80.−e, 77.84.Dy, 68.35.Bs

I. INTRODUCTION

In recent years ferroelectric (FE) materials with the perovskite ABO_3 structure have attracted attention owing to their prospective technological applications, e.g., actuators in MEMS/NEMS and nonvolatile random access memories (FeRAM).[1,2] As these applications are realized in complex components or thin film geometries whose size is now reaching extremely small dimensions down to several nanometers, where the effect of surfaces and interfaces can be critical, it has been drawing immense interest in the ferroelectricity in the vicinity of interfaces or surfaces.

The rapid change of the coordination number at a surface layer can significantly affect the ferroelectric and other distortions because the structural instability is related to the delicate balance between long-range Coulomb and short-range covalent interactions.[3,4] Thus, the surface structure of perovskites has been one of the central issues of ferroelectric materials and a lot of effort has so far been devoted. A number of studies on the variation of phases in $PbTiO_3$, which is a prototypical lead-base ferroelectric perovskite, have been carried out both theoretically and experimentally.[5–8]

The perovskite structure exhibits various lattice instabilities causing antiferrodistortive (AFD), antiferroelectric (AFE), and ferroelectric distortions, which in general compete with each other.[9,10] In bulk $PbTiO_3$ the AFD distortion is suppressed by the FE and does not appear in the FE tetragonal phase.[11] In the vicinity of a surface, however, this is no longer the case and the mixture of phases can emerge. In a recent presentation Bungaro and Rabe[12] studied the $PbTiO_3$ (001) surface structure by means of *ab initio* density functional theory (DFT) calculations and revealed that the surface termination significantly influences the surface polarization and that antiferrodistortive (AFD), antiferroelectric (AFE), and ferroelectric distortions coexist at the PbO-termination forming $c(2\times2)$ surface reconstruction, which agreed very well with a preceding experimental observation.[13]

Since the lattice of thin films, which are normally fabricated by epitaxial growth on a substrate, is subject to constraint of the substrate, it is necessary to investigate not only the influence of surface but also the effect of lateral strain. Especially $PbTiO_3$ shows the relatively large tetragonal ratio at the equilibrium, which should be closely correlated with the ferroelectric distortion.[14,15] This suggests that the ferroelectricity is eminently affected by both isotropic and anisotropic tangential strains. Nevertheless, the interplay between the FE/AFE/AFD distortions at the surface and lateral lattice parameter or in-plane strains has never been thoroughly investigated.

In this study we carried out *ab initio* (first-principles) DFT calculations to reveal the ferroelectricity of $PbTiO_3$ (001) surface placing a focus on the effect of lateral strain. Ferroelectric polarizations normal (out of plane) and parallel (in plane) to the surface are two special (ideal) cases. Although a phase with a superposition of the two polarizations should exist in reality and it may be difficult to separate them in experiment, it must be straightforward and scientifically reasonable to reveal the properties and structures of these special cases. The former case causes a depolarization field and requires a special treatment under the periodic boundary conditions, but was nicely investigated by Meyer *et al.*[16] We therefore focus only on in-plane polarization in this paper. Although it has been revealed that the PbO-terminated surface is the energetically most favorable in $PbTiO_3$ surface, we examine both TiO_2 and PbO terminations with the aim to elucidate the fundamental mechanism of the strain effect on the surface structure.

II. COMPUTATIONAL DETAILS

A. Methodology

Ab initio DFT calculations based on the projector augmented wave [PAW (Ref. 17)] method is conducted using the VASP package (Vienna *ab initio* simulation package[18,19]) with a plane-wave cutoff energy of 500 eV. The LDA (local density approximation) exchange correlation functional of the

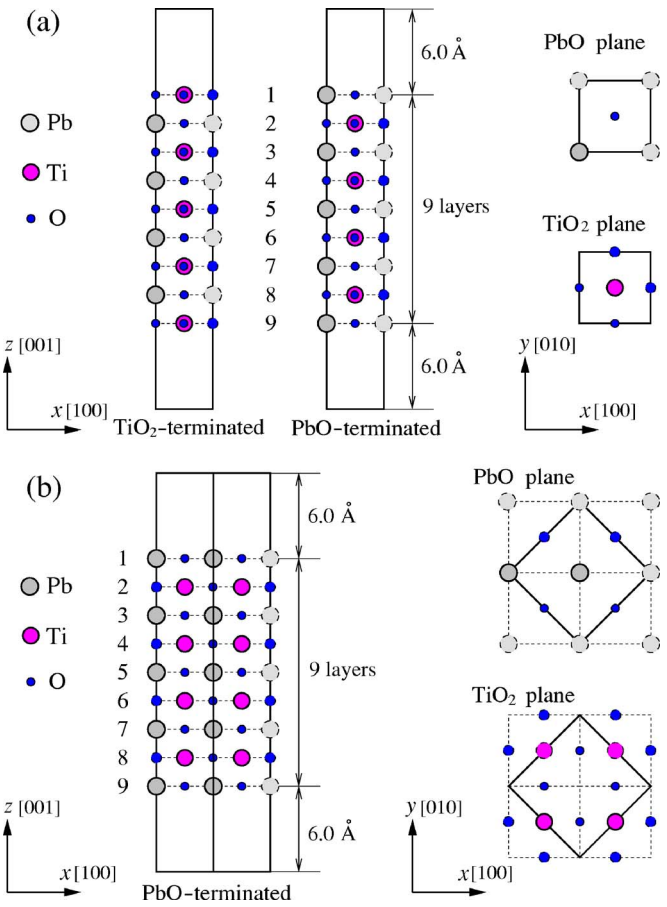

FIG. 1. (Color online) Simulation models of $PbTiO_3(100)$ surface. (a) (1×1) and (b) $c(2\times2)$ models. Solid boxes represent simulation supercells.

Ceperley-Alder form[20] is employed. The semicore Pb $5d$, and Ti $3s$ and $3p$ orbitals are included as valence states.

B. Models and simulation procedure

In this work, we study $PbTiO_3(001)$ surface models with both TiO_2 and PbO terminations using supercell setups for both terminations with slab geometries having nine atomic layers each (Fig. 1). For the PbO-terminated surface both (1×1) and $c(2\times2)$ periodicity models are employed to study FE-only and FE with coexisting AFD phases, respectively. The boundaries are periodic and the vacuum layers are set to 12 Å so that undesirable interaction of the surfaces through the vacuum is sufficiently avoided. The Brillouin-zone integrations are carried out with a $4\times4\times2$ Monkhorst-Pack[21] k-point mesh with a 0.2 eV Gaussian broadening for the (1×1) model and $3\times3\times2$ for $c(2\times2)$. Initially the atoms are arranged on the lattice points of the cubic perovskite structure with its theoretical lattice constant of $a=3.891$ Å. Then the atomic coordinates are fully relaxed with a mirror symmetry in the z direction to confine the ferroelectricity only in the lateral directions. To obtain FE/AFE/AFD configurations, the relaxation is started from slightly distorted configurations so that the systems possess proper symmetry of the aimed structure. The relaxation is performed under zero and nonzero lateral strain, until all the forces are less than 0.005 eV/Å. For the lateral strain, (a) isotropic $(\varepsilon_{xx}=\varepsilon_{yy}\neq0)$ and (b) [100]-uniaxial $(\varepsilon_{xx}\neq0, \varepsilon_{yy}=0)$ strain conditions are simulated. Note that in both cases the lattice relaxes along the z direction. The stress condition is therefore (a) $\sigma_{xx}=\sigma_{yy}\neq0$, $\sigma_{zz}=0$ and (b) $\sigma_{xx}\neq0$, $\sigma_{yy}\neq0$, $\sigma_{zz}=0$.

TABLE I. Polarization distortion, δ, in percentage of the lattice parameter ($a=3.891$ Å), at TiO_2- and PbO-terminated surfaces with (1×1) periodicity. The ordering in the leftmost column is the atomic layer number from the surface layer.

	TiO_2 termination				PbO termination			
	P[100]		P[110]		P[100]		P[110]	
Layer	TiO_2	PbO	TiO_2	PbO	TiO_2	PbO	TiO_2	PbO
1	2.29		2.58			13.48		12.10
2		3.40		3.64	4.75		5.26	
3	3.48		3.82			8.77		8.70
4		6.77		6.62	4.09		4.34	
5	3.81		4.04			8.05		7.93
Bulk	3.95	7.67	4.14	7.47				

III. RESULTS AND DISCUSSION

A. Unstrained structure

Here the ferroelectricity of unstrained films ($a=3.891$ Å) is shown. We introduce δ defined as follows to represent polarization distortion of each layer:

$$\delta_i=\begin{cases}[\bar{\delta}_i(\mathrm{Pb})-\bar{\delta}_i(\mathrm{O})] & (\mathrm{PbO\ layer}),\\ [\bar{\delta}_i(\mathrm{Ti})-\bar{\delta}_i(\mathrm{O})] & (\mathrm{TiO_2\ layer}),\end{cases} \quad (1)$$

$$(i=x,y)$$

$$\delta=\sqrt{\delta_x^2+\delta_y^2}, \quad (2)$$

where $\bar{\delta}_i$ is the layer-averaged atomic displacement relative to ideal lattice sites. Table I shows layer-by-layer δ of the (1×1) models with both terminations. Polarization directions both in [100] and [110] are calculated. Only the distortions of the top-half layers are shown because of the above-mentioned mirror symmetry imposing the identical distortions in the other half. For the TiO_2 termination, δ gradually decreases toward the surface layer while the opposite trend is found in the PbO termination, which manifests that the polarization distortion is suppressed by TiO_2-terminated surface and is enhanced by PbO term. This is consistent with the theoretical study by Meyer *et al.*[22] δ at layer 5 is close to the bulk value for both terminations indicating that our models have sufficient thickness to represent surface effects. The lateral ferroelectric distortions in both polarization directions are comparable in magnitude. The energy of the (1×1) ferroelectric surfaces listed in Table II

TABLE II. Energy of the [100]- and [110]-polarized FE phases in difference from paraelectric structure per unit (1×1) surface unit cell (in eV).

	TiO_2 termination	PbO termination
P[100]	−0.0219	−0.1607
P[110]	−0.0247	−0.1636

signifies that the polarization in [110] direction is preferred with a small energy advantage of 2.96 mJ/m^2 over [100] polarization in both terminations.

As for the PbO-terminated $c(2\times2)$ model, several (meta)stable structures with the coexistence of FE and AFD are found as schematically depicted in Fig. 2. In this phase the polarization directions of unit cells are not identical; the polarizations are deviated from their average directions ([100] or [110]) clockwise or counterclockwise, which is clearly due to the contribution of AFE distortion, as was demonstrated in Ref. 12 This phase will be denoted as "FE +AFD (coexisted) phase" hereafter in this paper for brevity. The energy, the polarization distortion, and the AFD rotation in this phase are listed in Table III. Here, we introduced the polarization direction angle,

$$\phi = \tan^{-1}(\delta_y/\delta_x). \tag{3}$$

ϕ_{ave} is the averaged polarization direction (0° in P[100] and 45° in P[110], thus $\phi-\phi_{ave}$ denotes the strength of polarization rotation induced by AFE. It should be noted that in our notation δ represents the distortion by the FE and AFE. As for θ, we use the same definition as in Ref. 12 and take the rotation angle of the oxygen squares in the TiO_2 planes. An important finding here is that the P[110]-*A* structure, average polarization in the [110] direction, is energetically the most favored with the nontrivial energy advantage of about 0.037 eV per (1×1) surface unit cell (39.7 mJ/m^2) to the other metastable phases. This was not yet considered in Ref. 12 where only P[100] was investigated. Although the magnitude of the AFD rotation is almost comparable among the three phases, the magnitude of $\phi-\phi_{ave}$ of PbO layers in P[110] is more than twice larger than that in P[100] indicating that AFE is strong when the average polarization is in [110].

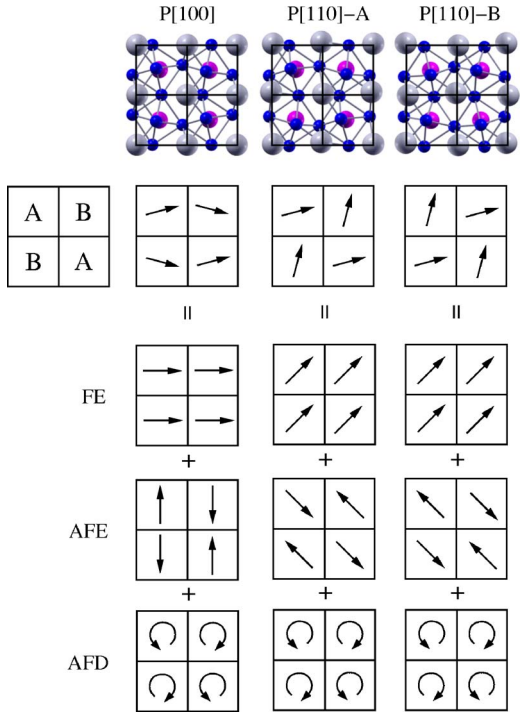

FIG. 2. (Color online) Atomic structure of (meta)stable phases at PbO-terminated $c(2\times2)$ surface. Only the first two layers at surface are depicted in the top figures. Arrows indicate FE and AFE distortions of the first PbO layer and AFD rotation of the adjacent TiO_2 layer.

TABLE III. FE distortion and AFD rotation structure at the unstrained PbO-terminated $c(2\times2)$ surface. ϕ is for the shaded cell in Fig. 2. Energy is as the difference from PE phase in eV per (1×1) surface unit cell. δ is in percentage of the lattice parameter, $a=3.891$ Å. ϕ and θ are those of cell *A* in Fig. 2 in degree.

		P[100]	P[110]-*A*	P[110]-*B*
		Layer ($\phi_{ave}=0°$)	($\phi_{ave}=45°$)	
Energy		−0.2323	−0.2695	−0.2322
δ	1	12.22	10.68	10.63
	2	4.18	4.36	4.22
	3	6.70	6.35	7.00
	4	3.88	4.10	4.05
	5	7.69	7.29	7.29
$\phi-\phi_{ave}$	1	13.9	−36.1	31.9
	2	−6.8	1.1	4.4
	3	−5.4	24.7	−21.4
	4	1.0	−0.8	−0.8
	5	5.0	−18.2	−16.6
θ	2	11.0	10.6	11.2
	4	−0.3	−0.4	−0.1

B. Influence of isotropic strain

The polarization distortion per area must be the relevant value to represent the response of polarization to strain (recall that polarization of bulk material is defined as dipole moment per volume). Change in the polarization distortion, $\delta'=\delta/A$ (A is surface area), with respect to lateral isotropic strain in the (1×1) models is shown in Fig. 3. In this paper we write $\varepsilon=\varepsilon_{xx}+\varepsilon_{yy}$. We explore strain up to 20%, which may be beyond the experimentally accessible region (note that strain of 20% means 10% change of lattice parameter). However, it would be instructive for understanding the fundamental physics of the material properties at surfaces. Here the polarization direction is always in the [110] direction because we confirmed that [100]-polarized structure has larger energy under nonzero isotropic strain as well. In the

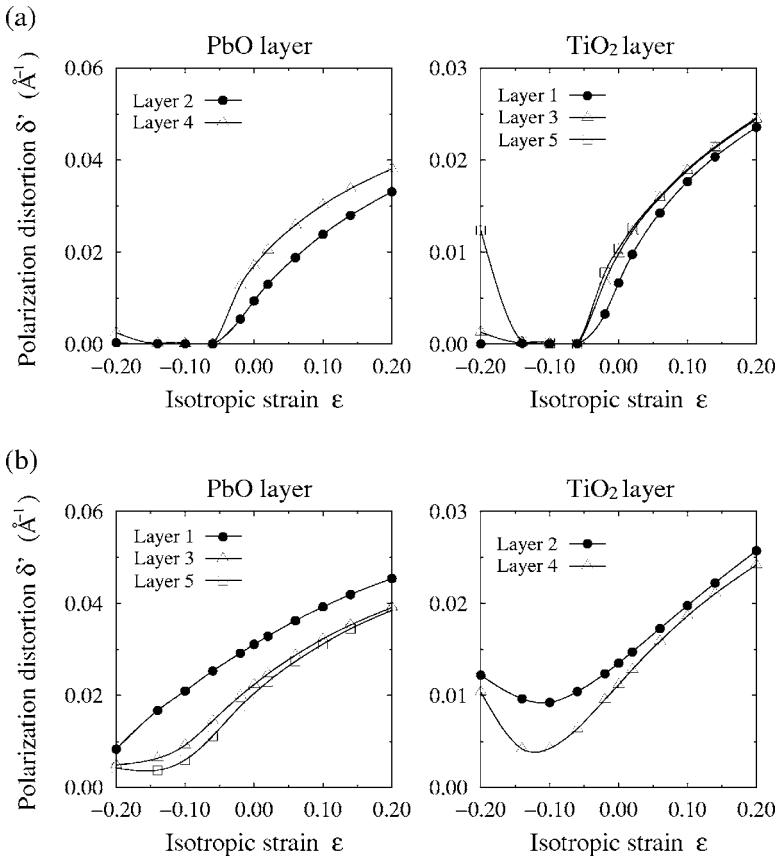

FIG. 3. Polarization distortion per area, δ', as a function of isotropic strain, ε, in the (1×1) models. (a) TiO_2-terminated surface and (b) PbO.

case of TiO_2 termination δ' increases smoothly with increasing (tensile) strain, showing the enhancement of ferroelectricity by tangential stretch. On the other hand, ferroelectricity is suppressed under compression and vanishes at $\varepsilon=-0.06$, indicating the existence of the critical compressive strain for ferroelectricity. When the surface is further compressed the ferroelectricity emerges again. This is accounted for by FE enhancement in bulk under extreme compression reported by Kornev.[23] The response of δ' to the tangential strain in the PbO-terminated surface is similar. Under compression, however, δ' does not vanish because of the enhancement of FE distortion by PbO termination.

The FE distortion and relatively large tetragonality in $PbTiO_3$ originates in the partially covalent short-range Pb-O bond with the hybridization between the Pb $6s$ and O $2p$ states.[14,15] Change in the atomistic and electronic configurations in response to the isotropic strain at the surface layer of the PbO-terminated (1×1) model is shown in Fig. 4(a). At no strain and under tension, $\varepsilon\geqslant0$, localization of charge density between the center O and the corner Pb atoms is found indicating a strong covalent bonding. As the strain grows the distance between the Pb and O atoms decreases only slightly from 2.28 Å at $\varepsilon=0$ to 2.20 Å at $\varepsilon=0.20$. The strong Pb-O covalent bonding is therefore the major cause of the significant increase in δ' by tension. Although the displacement is relatively small, a similar behavior is found in the FE distortion of TiO_2 layers. Figure 4(b) displays the charge density localization between Ti and O under tension, which indicates covalent bondings enhancing polarization.

Change in the structure of $c(2\times2)$ P[110]-A phase of the PbO-terminated surface is shown in Fig. 5. The response of the polarization distortion (δ') to the variation of the isotropic strain is similar to that in the (1×1) model; the polarization is enhanced by tension and suppressed by compression. The AFD rotation has a nature of the opposite trend [see dashed lines in Fig. 5(b), which are the results of AFD-only phase]. In the FE+AFD coexisted phase, FE and AFD compete with each other, resulting in the AFD rotation being more suppressed by the FE distortion under tension and the FE being more weakened by the AFD under compression.

C. [100] uniaxial tension and compression

Tensile and compressive uniaxial strain in [100] changes the aspect ratio of the $PbTiO_3$ lattices, which can cause variation in the in-plane polarization direction as well as the magnitude. Changes in the polarization distortion (δ') and direction (ϕ) at the (1×1) surfaces with respect to ε_{xx} are shown in Figs. 6 and 7. In both terminations the polarization direction rotates toward [100] under tension and [010] under compression due to the preference of the polarization along the longer axis of rectangular lattices. Although the polarization distortions differ with the layer, their directions are identical in all the layers. While the evolution of δ' with growing tensile strain is similar to that in the case of isotropic tension, the distortion is less suppressed under compression. No critical strain for ferroelectricity is found regardless of the termination layer. In the PbO-terminated surface, the change of δ' shows slight a wiggle around $\varepsilon_{xx}=0$, which is obviously concomitant to the polarization rotation.

The polarization direction and distortion in the FE+AFD coexisted phase of the $c(2\times2)$ PbO-terminated

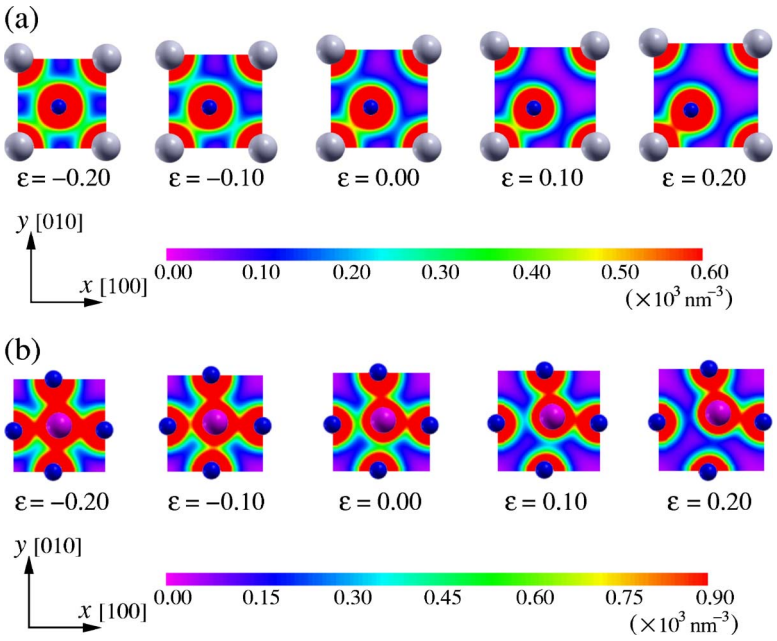

FIG. 4. (Color online) (a) Change in atomistic and electronic configurations at the surface PbO layer of the (1×1) model under isotropic strain. Corner gray spheres are Pb atoms and center blue is O. Only valence charge density is presented by color. (b) Same figure for the adjoining TiO_2 layer (second layer). Center purple sphere is Ti. The window is taken so that the O atoms (blue spheres) are on the edges, meaning that the windows of (a) and (b) do not correspond with each other.

model is shown in Fig. 8. Although the polarization distortion as a function of [100] strain is quite similar to that of the (1×1) model, the FE direction behaves differently: ϕ differs among the layers. The surface layer prefers to have polarization in the [110] direction and the adjacent layer is slightly affected. This result suggests that different polarization directions depending on the distance from the surface can be observed at the $PbTiO_3$ surface subjected to a high uniaxial strain.

Figure 9 shows a change in the atomistic and electronic configurations at the surface layer of the PbO-terminated models. In the (1×1) model, the center oxygen atom is shifted toward a corner Pb with a strong covalent bond (α) and two equivalent weak bonds (β and γ) at $\varepsilon=0.0$. When a strain is applied in the x direction, the oxygen immediately moves towards either of the equivalent bonds to form two strong bonds; α and β under tension or α and γ under compression. This mechanism, which is also found in the TiO_2-terminated surface, explains the polarization rotation very sensitive to the uniaxial strain in the (1×1) periodicity. On the other hand, the $c(2\times2)$ PbO-terminated surface has the different bond structure; oxygen atoms are shifted in dif-

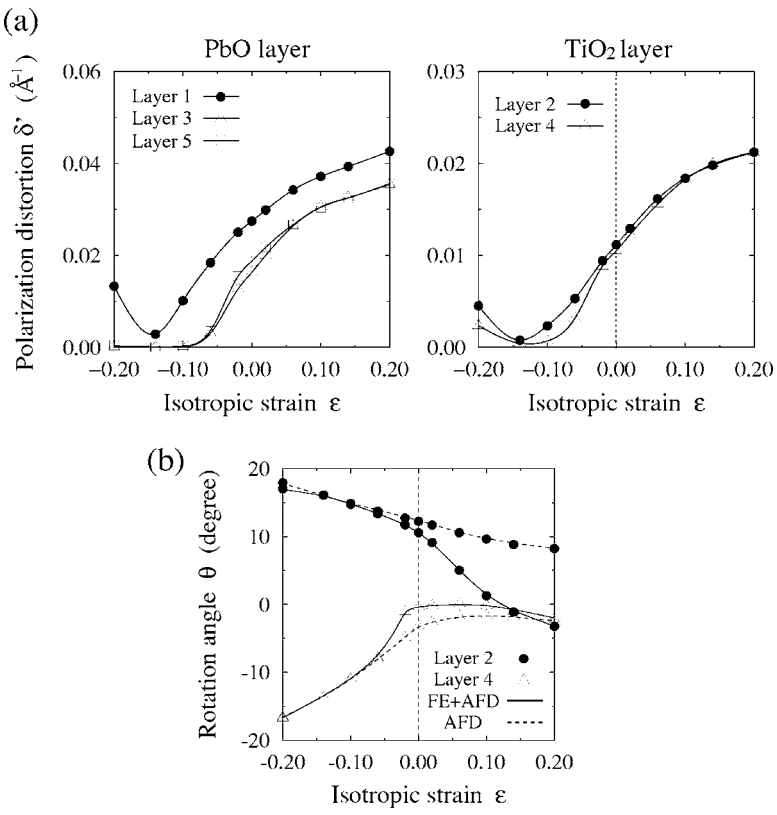

FIG. 5. Change in structure of $c(2\times2)$ PbO-terminated surface as a function of isotropic strain, ε; (a) polarization distortion per area, δ', and (b) antiferrodistortive rotation angle, θ. Dashed lines in the bottom figure represents the results of AFD-only phase for comparison, where FE polarization is artificially frozen out.

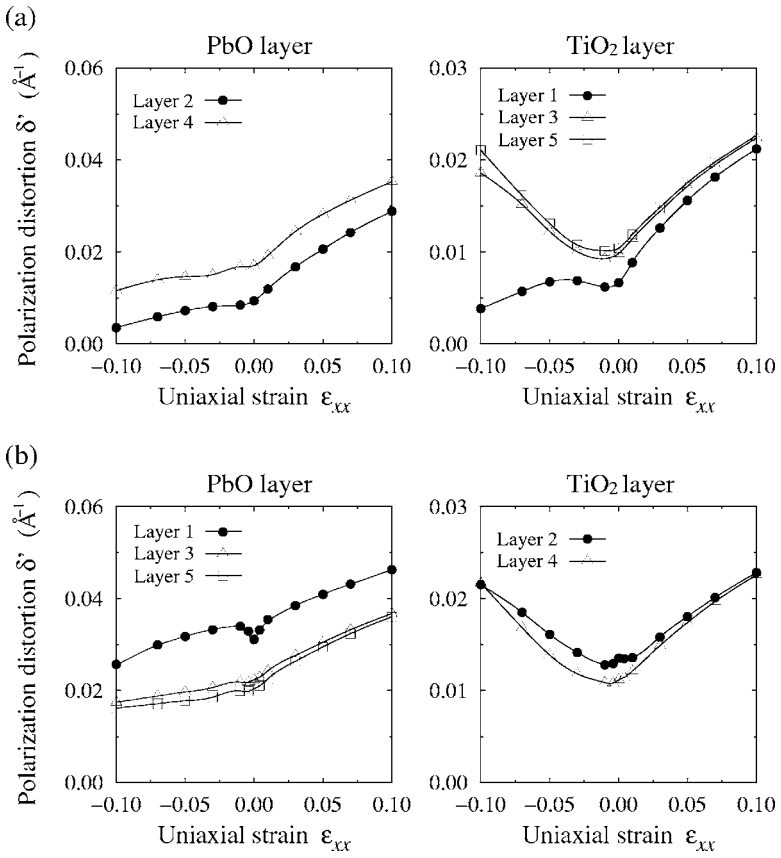

FIG. 6. Polarization distortion per area, δ', of (1×1) surface as a function of uniaxial strain ε_{xx}.

ferent directions in the lattices A ([010]) and B ([100]), each forming two strong covalent bonds with the nearest Pb atoms. The bond structure in the lattice A does not immediately change when a small uniaxial tension is applied. At relatively high strain ($\varepsilon_{xx}>0.07$) the shift of the oxygen occurs with the break of γ bond followed by the construction of β bond, consequently forming [100] polarization in both lattices. It is worth noting that the [100]-polarized structure becomes energetically almost identical to the [100]/[010] mixed polarization at a lower strain, $\varepsilon_{xx}\sim0.05$, which indicates the existence of small energy barrier between those structures for the bond reconstruction of β and γ bonds. In contrast, the mixed polarization is always more favored than [010] under compression despite the increase in the tetragonal ratio. This is because compression is applied keeping L_y (lattice parameter in the y direction) in our calculation, which does not lead to bond breaking required for the reconstruction of polarization structure.

D. Energy difference between phases

Now we examine the energy difference between the most favored phase shown so far and metastable ones to discuss the stability of the phases because the FE(+AFE) and AFD structures can be subject to change due to the infusion of external energy such as finite temperatures. The potential energies per (1×1) surface unit cell of the phases (PE, FE, AFD, and FE+AFD) as a function of the isotropic strain and the uniaxial one are presented in Fig. 10. At zero strain, the energy difference between FE and PE is only 0.05 eV at the TiO_2 termination, representing that the FE phase is easily shifted to PE, while at the PbO termination the FE+AFD phase is more stable with the energy gain of about 0.25 eV from FE or AFD. In both TiO_2- and PbO-terminated surfaces, the energy difference between the PE and FE phases is increased by the tensile strain both in the isotropic and the uniaxial strains, meaning the tension stabilizes the FE

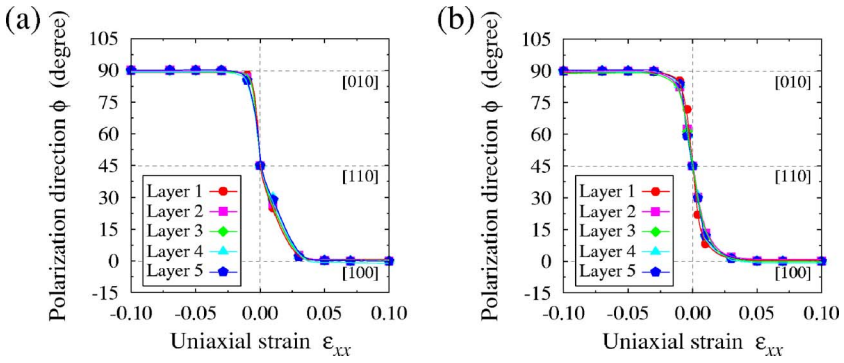

FIG. 7. (Color online) Direction of polarization distortion, ϕ, of (1×1) as a function of uniaxial strain ε_{xx}. (a) TiO_2-terminated surface and (b) PbO.

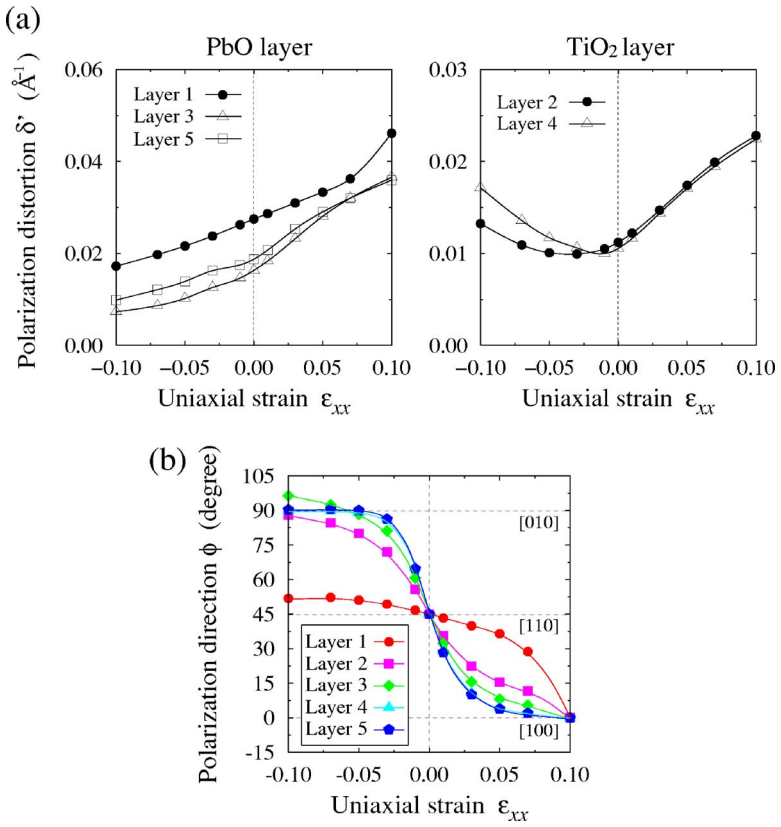

FIG. 8. (Color online) Change in structure of $c(2\times2)$ PbO-terminated surface as a function of uniaxial strain ε_{xx}; (a) polarization distortion per area, δ', and (b) polarization direction, ϕ.

polarization. In the PbO termination, the energy of the most favored FE+AFD state becomes close to that of the FE state under tension and to AFD under compression. This is consistent with the fact that tension (compression) suppresses the AFD (FE), resulting in smaller energy gain by the phase shift from AFD+FE to FE (AFD) under tension (compression). The relatively high energy difference from the remaining two phases indicates that the phase is likely confined to FE+AFD or FE under tension and to FE+AFD or AFD under compression.

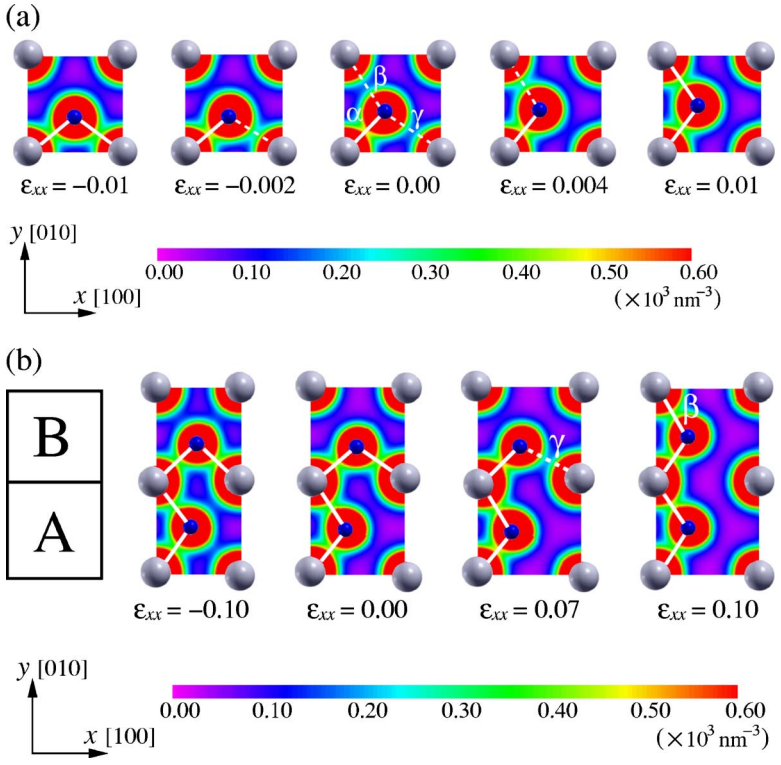

FIG. 9. (Color online) Change in atomistic and electronic configurations at the surface PbO layer under uniaxial strain. (a) (1×1) and (b) $c(2\times2)$ models.

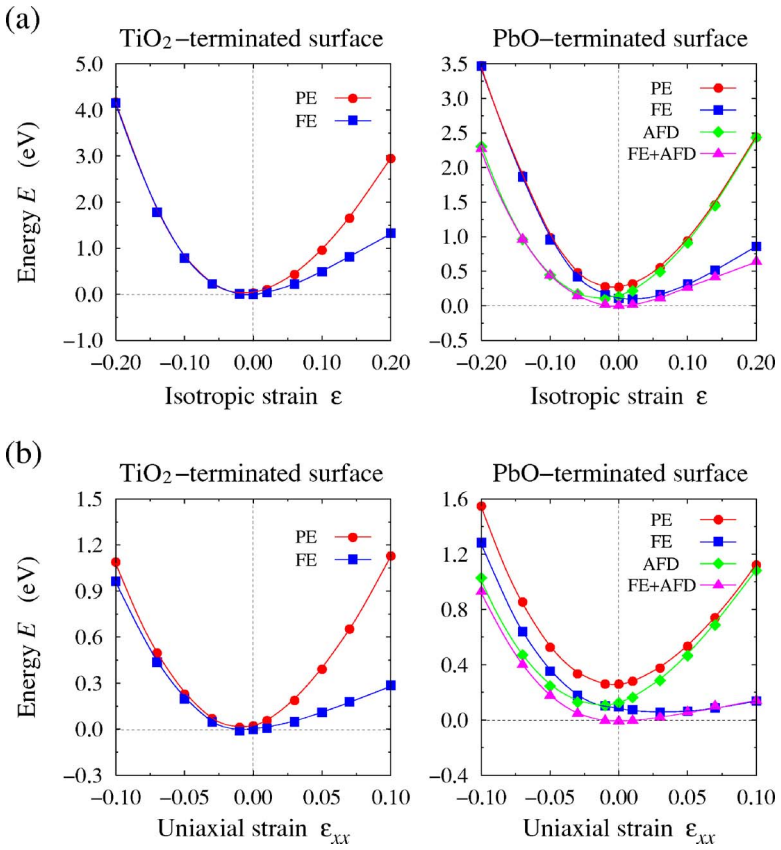

FIG. 10. (Color online) Relative energy per (1×1) surface unit cell as a function of (a) isotropic strain ε and (b) uniaxial strain ε_{xx}.

IV. CONCLUSION

We have performed *ab initio* DFT calculations to reveal the $PbTiO_3(001)$ surface structure having FE (ferroelectric) polarization parallel to the surface and its response to tangential strain. Excellent agreement with previous studies[12,22] is found in the surface structure with FE distortions which depends on the terminations, suppressed by TiO_2 termination and enhanced by PbO, and also in the structure of the FE and AFD (antiferrodistortive) coexisted phase. We find, however, the ferroelectricity in the [110] orientation is the more stable phase in both TiO_2 and PbO terminations than the [100]-oriented FE phase. The energy difference between the two FE orientations is nontrivial at $c(2\times2)$ PbO-terminated surface with FE+AFD coexisted structure.

We demonstrate the strong influence of lateral isotropic strain on the FE and AFD distortions: The ferroelectricity is enhanced by lateral tensile strain while it is suppressed by compression. At TiO_2 terminated surface, ferroelectricity disappears when the compressive strain reaches a critical value. In the PbO termination, however, ferroelectricity is not suppressed by the surface and thus polarization distortion does not vanish under high compressive strain. These results indicate the surface FE and AFD distortions can be tuned by the lattice constant of the substrate on which the $PbTiO_3$ film is epitaxially grown.

Furthermore we examine the effect of uniaxial [100] strain is examined and find the rotation of ferroelectric polarization direction, which prefers to be along the longer axis of rectangular lattices. While the response is sharp at the (1×1) reconstructed surfaces, the surface layer exhibit [110]-oriented FE polarization up to relatively high tensile and/or compressive strains at the PbO-terminated $c(2\times2)$ surface, resulting in the variation of polarization directions among the layers.

From the analysis of energy difference between the polarized and paraelectric (PE) phases, we manifest that the tensile strain stabilizes the FE polarization in both terminations. Under compression the energy difference is very small, meaning that the surface structure is easily shifted to nonpolar phase where only the AFD distortion may exist.

ACKNOWLEDGMENTS

The authors acknowledge financial support for two of the authors (Y.U. and T.K.) from the Grant-in-Aid for Scientific Research of Japan Society of the Promotion of Science (JSPS, Grants Nos. 18760082 and 16106002), the Center of Excellence for Research and Education on Complex Functional Mechanical Systems (COE program of the Ministry of Education, Culture, Sports, Science and Technology of Japan) and Mechanical Engineering Research Laboratory, Hitachi Ltd, and for C.E. from the German Research Foundation (project EL 155/7-1 in the DFG priority program SPP 1157 "Integrated electroceramic functional structures") and the European Commission [Contract No. NMP3-CT-2005-013862 (INCEMS)].

[1] J. F. Scott, *Ferroelectric Memories* (Springer, Berlin, 2000).
[2] R. Ramesh, *Thin Film Ferroelectric Materials and Devices* (Kluwer Academic, Boston, 1997).
[3] R. Resta, M. Posternak, and A. Baldereschi, Phys. Rev. Lett. **70**, 1010 (1993).
[4] W. Zhong, R. D. King-Smith, and D. Vanderbilt, Phys. Rev. Lett. **72**, 3618 (1994).
[5] R. D. King-Smith and D. Vanderbilt, Phys. Rev. B **49**, 5828 (1994).
[6] P. Ghosez, E. Cockayne, U. V. Waghmare, and K. M. Rabe, Phys. Rev. B **60**, 836 (1999).
[7] G. Shirane and R. Pepinsky, Acta Crystallogr. **9**, 131 (1956).
[8] A. M. Glazer and S. A. Mabud, Acta Crystallogr., Sect. B: Struct. Crystallogr. Cryst. Chem. **34**, 1065 (1978).
[9] M. E. Lines and A. M. Glass, *Principles and Applications of Ferroelectrics and Related Materials* (Clarendon, Oxford, 1977).
[10] F. Jona and G. Shirane, *Ferroelectric Crystals* (Dover, New York, 1993).
[11] A. García and D. Vanderbilt, Phys. Rev. B **54**, 3817 (1996).
[12] C. Bungaro and K. M. Rabe, Phys. Rev. B **71**, 035420 (2005).
[13] A. Munkholm, S. K. Streiffer, M. V. Ramana Murty, J. A. Eastman, C. Thompson, O. Auciello, L. Thompson, J. F. Moore, and G. B. Stephenson, Phys. Rev. Lett. **88**, 016101 (2001).
[14] R. E. Cohen, Nature **358**, 136 (1992).
[15] Y. Kuroiwa, S. Aoyagi, A. Sawada, J. Harada, E. Nishibori, M. Takata, and M. Sakata, Phys. Rev. Lett. **87**, 217601 (2001).
[16] B. Meyer and D. Vanderbilt, Phys. Rev. B **63**, 205426 (2001).
[17] P. E. Blöchl, Phys. Rev. B **50**, 17953 (1994).
[18] G. Kresse and J. Hafner, Phys. Rev. B **47**, 558 (1993).
[19] G. Kresse and J. Furthmüller, Phys. Rev. B **54**, 11169 (1996).
[20] D. M. Ceperley and B. J. Alder, Phys. Rev. Lett. **45**, 566 (1980).
[21] H. J. Monkhorst and J. D. Pack, Phys. Rev. B **13**, 5188 (1976).
[22] B. Meyer, J. Padilla, and D. Vanderbilt, Faraday Discuss. **114**, 395 (1999).
[23] I. A. Kornev, L. Bellaiche, P. Bouvier, P. E. Janolin, B. Dkhil, and J. Kreisel, Phys. Rev. Lett. **95**, 196804 (2005).